The Femtosecond Micromachining of Plasma Waveguides

S. Abuazoum[1)], S. M. Wiggins[2)],K.Hart[2)] ,S.Abuzareba[1)]
1) Dept of Physics, University of Misurata, Libya
2) SUPA, Dept of Physics, University of Strathclyde, Glasgow, UK
E-mail of corresponding: saliaazoum@gmail.com

Abstract: This paper investigates the creation of aluminium oxide plasma waveguides that are suitable for the guiding of high power femtosecond laser pulses in non-linear laser-plasma interaction experiments. Circular waveguides were micromachined using a femtosecond laser system to ablate in a controlled manner the surface of two aluminium oxide plates. Creating a semi-circular profile in each plate allows a circular capillary channel to be formed. Two waveguides were constructed: each is 4 cm in length but with a different capillary diameter profile. The first waveguide was a linear (straight) waveguide with a constant diameter of 288 μm and the second featured a taper in its diameter from 289 – 232 μm.

Introduction

The work presented in this paper was carried out in the TOPS laser laboratory of the University of Strathclyde. It involved the femtosecond micromachining of aluminium oxide plasma waveguides, which can be used in experiments such as laser wakefield acceleration [1] and Raman amplification [2]. Plasma accelerators have ability to sustain extremely large acceleration gradients. Conventional radio-frequency linear accelerators cannot allow such acceleration gradients, which is partly due to the breakdown that occurs on the walls of the structure. Conventional linear accelerators are currently limited to 100MVm-1 [3] and required great distances to attain this, making them a less efficient method of acceleration. Acceleration gradients in plasma however, can reach the order of 100GVm-1 which is three orders of magnitude greater than conventional linear accelerators [3]. The fundamentals of plasma-based acceleration involve the harnessing of a plasma wave produced by an intense laser pulse propagating through plasma [4].

This drives collective oscillations of plasma electrons through a background of plasma ions [3] and the pulse is assumed to propagate close to the speed of light. The electron motion in the plasma induces charge separation resulting in high electric fields and a strong restoring Coulomb force which are responsible for driving the plasma electron oscillation. Therefore, particles gain energy through an excited longitudinal plasma wave which is the basis of accelerating particles to relativistic energies [5]. An effective method of generating an excited plasma wave is through laser wakefield excitation. The original concept and theory of laser wakefield acceleration was devised by Tajima and Dawson in 1979 [4]. The laser pulse propagates in the plasma close to the speed of light, causing the plasma electrons to oscillate at the

frequency of the laser, known as "quiver motion". This gives rise to the ponderomotive force of the laser pulse which excites the plasma, pushing electron aside and creating a charge separation. This is shown in Figure 1 which illustrates the wake created by the laser pulse.

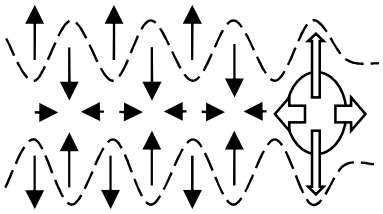

Figure 1: The ponderomotive force (large arrows) pushes aside electrons resulting in strong electrostatic forces (13) that drive electrons back into the wake (shown as small arrows) creating an acceleration gradient.

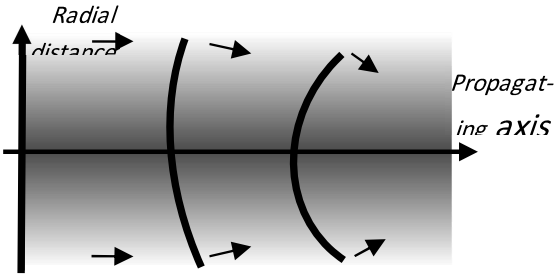

Figure 2 – Schematic diagram portraying how a plane wavefront becomes convex after propagating through a medium with a refractive index that decreases with radial distance.

This plasma wakefield [6] is responsible for high acceleration gradients and is able to accelerate electrons to near 100s of MeV in just a few mm and even 1 GeV using a 33 mm long discharge capillary waveguide [7]. The SILIS group at The University of Strathclyde, have constructed a fully operational laser wakefield accelerator (ALPHA-X beam line) which generates ultra-relativistic electron beams driven by a 30 TW femtosecond laser system [8]. Many applications of high-intensity laser pulses require optical guiding in order to increase the interaction length with the laser radiation [9]. The distance a beam of radiation can maintain its high intensity is limited fundamentally by diffraction [4]. Therefore, waveguides are extremely important for channelling a beam in order to obtain greater propagation distances. Plasma waveguides operate by forming a plasma with a refractive index that decreases with radial distance from the propagation axis [9]. This causes the phase velocity to increase with radial distance and so the wavefront of an initially-plane wave will become convex as shown in Figure 2. The result of this refractive index guiding is the focusing of the beam which counteracts diffraction and ionization-induced refraction [9].

2 Theory

a) Laser Ablation and Micromachining

Laser ablation involves the removal of material from a substance through the laser induced excitation and ejection of atoms, ions and molecules from the material's surface. A technique that exploits the ablation characteristics of short-pulse lasers is laser micromachining. This is used to minimise the thermal and mechanical defects of a substrate produced through conventional methods such a drilling. The ablation of

materials using short-pulse lasers is becoming a favourable method of surface rendering.

In order to remove an atom from a solid using a laser pulse, the energy of the pulse should be greater than the binding energy of the atom [10]. The electrons of the material absorb the high energy from the pulse and as a result are ejected from the target. The charge separation produced will create an electric field which in turn, entices the ions to be pulled out of the target. Simultaneously, the ponderomotive force of the laser field in the outer layer of the material forces electrons back into the target which creates an acceleration gradient for the ions. The ions are then accelerated into the target and are responsible for the ablation of the material. During laser ablation, dense hot plasma is created near the target surface as the material is ionized. This plasma absorbs energy from the laser pulse.

when the ion density is high as well as receiving evaporating material at its inner surface [9]. The absorbed energy in the plasma is converted into thermal energy which then completely ejects material and so allows surface ablation.

b) Femtosecond Laser Ablation

Femtosecond laser pulses can machine any material with good spatial resolution and quality [10]. For machining dielectrics like alumina, the primary absorption mechanism is multi-photon absorption [11], made possible by the high intensity (~1014 – 1015 Wcm-2) of the femtosecond laser pulse. However, for use in large industries, femtosecond laser ablation is expensive due to the advanced optics required in the laser system.

Femtosecond pulses deposit all their energy on a timescale shorter than the electron-phonon relaxation time which is typically around 0.5 – 5 ps. This creates a very high temperature gradient in material with virtually no heat diffusion away from the irradiated region during the rapid melting and ablation phase [12]. The thermal diffusion length is given by:

$$L_{diff}=2((\kappa\tau_L)/(\rho C_p)) \quad [1]$$

which is negligible in comparison to the skin depth for □L ~ 100 fs . This produces the very clean machining edge, as seen in the example of Figure 3(a), with very a small heat-affected zone (shown as the light discolouration around the hole) around the ablated region.

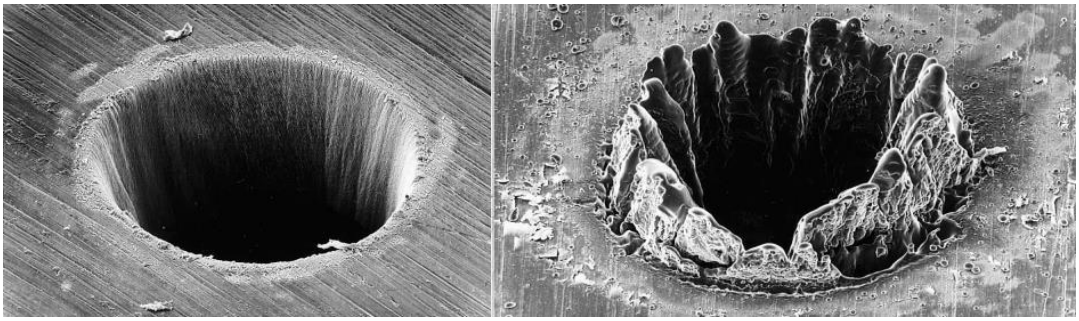

Figure 3 – shows the (a) femtosecond and (b) nanosecond ablation of 100μm thick steel foil where the heat affected zone considerably more significant in the nanosecond regime

From Figure 3a, it is clear that the femtosecond beam produces minimal damage as the heat affected zone (shown as the light discolouration around the hole) is much less than that of the nanosecond laser shown in Figure 3b.

c) Nanosecond laser ablation

For nanosecond pulses, there is a large melt front and sputtered material appears in both vapour and liquid phases. The longer pulses of the nanosecond laser result in significant thermal diffusion of heat away from the irradiated region during the irradiation time itself. This reduces the temperature gradient (the pulse duration is also much longer than the electron-phonon relaxation time) and leaves a visible corona around the ablated area which can be clearly observed in Figure 3(b). A significant problem that occurs during nanosecond laser ablation is the liquid phase which is created along the diffusion length as the material "melts". The pulse does not have enough energy to evaporate the liquid, and so the material cools and leaves and uneven and jagged ablated region (Figure 3b).

d) Plasma Waveguide

A plasma waveguide [13] serves as a cylindrical cavity in which to confine plasma and guide a laser pulse. When plasma is harnessed within the waveguide, a thermal gradient is created where the highest temperature is located through the centre of the cylindrical channel along the axis of propagation. The refractive index will be highest at the centre of the channel and lower towards the walls of the cavity. The refractive index of plasma is given by:

$$\eta=\sqrt{(1-(N_e e^2)/(m_e \epsilon_0 \omega^2))} \qquad [2]$$

Where, N_e is the electron density, ω is the angular frequency of the radiation, m_e is the rest mass of the electron and ϵ_0 is the permittivity of the plasma [4].

A plasma waveguide consists of two sections which are machined to create a semi-circular profile along the length of each side. Figure 4 illustrates each machined side of the capillary.

The waveguides comprise of two aluminium oxide plates, each 4 cm long. The two plates are secured together to create the waveguide which is shown in Figure 4.

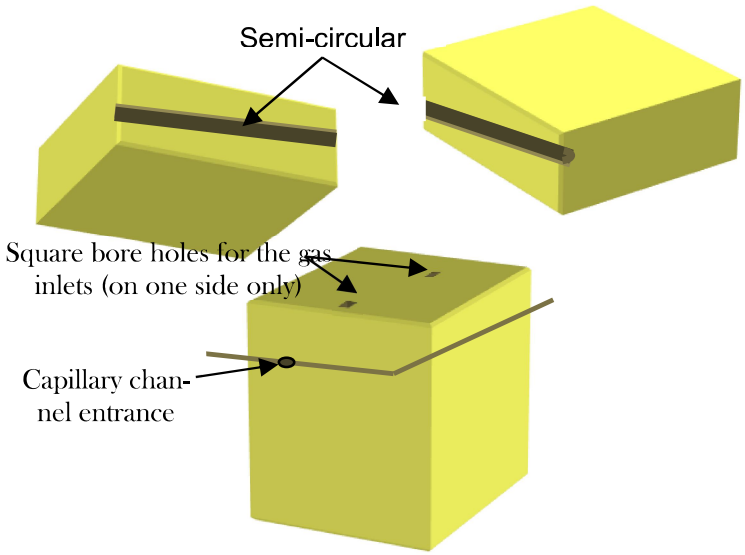

Figure 4 – Depiction of the plasma waveguide with a circular entrance to the channel and two gas inlet holes that connect to the cylindrical channel through the capillary.

3 Experimental Setup

The Strathclyde Electron and Terahertz to Optical Pump Source [14] uses high-power femtosecond lasers for a number of research applications. The laser system used in this work is a kHz repetition rate Ti:Sapphire (titanium-doped sapphire) femtosecond laser system. With suitable focusing of the laser beam, the intensity can reach 1015 Wcm-2. In order to perform the micromachining process, the femtosecond laser pulses are guided through a series of optics and focused on the target sample which is mounted in a holder. The basis set up is shown in Figure 5 which displays the femtosecond laser beam line and the HeNe laser beam line. The HeNe laser was used as a means of alignment for the femtosecond laser.

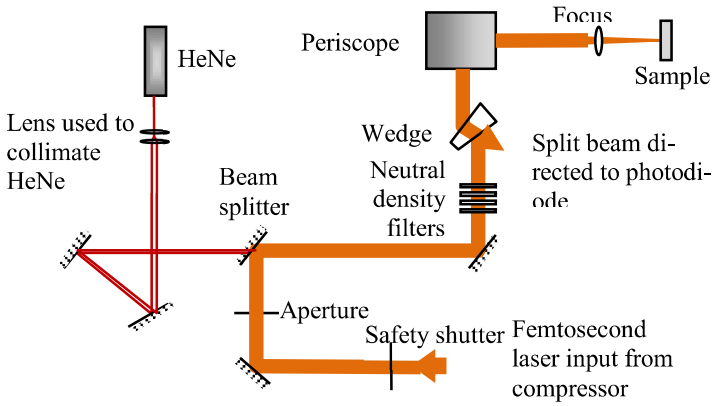

.

Figure 5 – Set up of the femtosecond laser beam directed onto the sample surface for micromachining. The femtosecond laser beam is shown as the thicker beam line and the helium neon laser beam is the narrower beam which is used to align the femtosecond beam.

In order to create a plasma waveguide, a micromachining station was set up, in which a capillary would secured in a holder at the end of the femtosecond beam line in order to be machined. The capillary holder is mounted on a translational stage which is used for machining a specified path across the capillary. The micromachining set up consists of the X, Y and Z-motorized, linear translational stages of the machining process. The machining is controlled by the XPS motion controller and during operation, it will reciprocate independently along the X and Y-translational stages. The lens on the Z-translational stage is positioned before machining begins in order to focus the beam.

Throughout the machining process, the Z-translational stage will remain stationary. The motion controller used to command the translational stages is a Newport XPS which is based on the TCP/IP internet connection protocol [15].

TCP provides a reliable point-to-point communication channel in which a process will not be disrupted by "blocking" any pending commands until the process is complete. The micromachining process duration can range from a few minutes, to several hours and so reliability is essential to limit the wastage of samples. Another method of ensuring the equipment remains fully functional during operation is the use of a photodiode. It is used to monitor the energy of the laser and if it falls below a predetermined threshold, the laser output is automatically terminated and the command execution is halted until the issue is resolved.

During micromachining, the intensity of the laser pulse remains constant, and therefore the machining process relies on the movement of the controller. The velocity of the controller is proportional to the depth of the ablated area of the sample, and so the controller is programmed to define a position and velocity for each stage of the process.

Capillary Machining Trajectories

a) Straight Capillary

To create a straight capillary channel, a program was written that would complete a trajectory at a constant velocity straight up the centre of the capillary along the Y-axis, then reposition along the x-axis before returning back down the y-axis. This trajectory loop is repeated along the set width of the channel until the required amount of material has been removed. The trajectory path is shown in Figure 6.

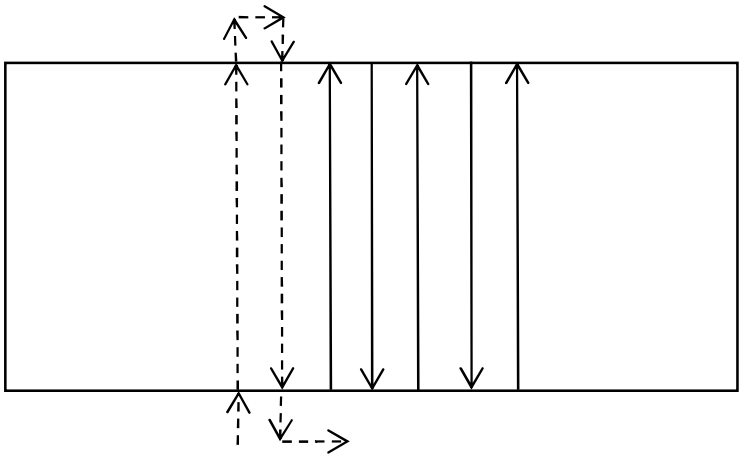

Figure 6 – Trajectory of the x and y-translational stages for the machining of a straight capillary The dashed line indicates a complete "round trip" which *is repeated across the width of the capillary channel.*

During the transition of each loop, the velocity of the Y-trajectory was altered to enable it to progressively slow down from the edge of the profile to the centre, and then again speed up towards the opposite edge of the profile. This meant that the laser would ablate a larger amount of material in the middle of the profile, and gradually ablate less towards each side to the channel. This whole process was repeated until a smooth, symmetrical semi-circular profile is created. The machining was repeated for the other side of the capillary and the two sides were glued together to create a straight, cylindrical plasma waveguide.

b) Tapered Capillary

In order to create a tapered capillary, both sides of the capillary were machined at the same time using the XPS motion controller. The XPS controller was programmed to complete a PVT (position, velocity, time) trajectory which is generated with the continuous movements of the MultipleAxes group's positioners over several time periods [15]. The trajectory across the two sides of the capillary is shown in Figure 7 with one "round trip" indicated by the dashed line.

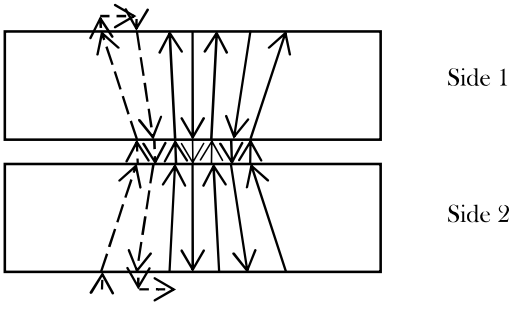

Figure 7 – Trajectory for micromachining both sides of the capillary simultaneously

The trajectory is much more complicated for machining the tapered capillary than for the straight capillary. The motion controller must control both the X and Y-axis trajectories simultaneously in order to obtain a smooth taper. The dashed line shown in Figure 7 represents one "round trip" of the controller. From below the bottom left hand side of side 2, the controller is accelerated from rest along the Y-trajectory before it reaches the edge of the capillary. It will continuously accelerate up the length of side 2 until the trajectory lies mid-way between side 1 and 2 where it will begin to decelerate. It will continue to decelerate along the length of side 1 until it comes to rest once it has cleared the top edge. Simultaneously, the X-trajectory will also advance back and forth along the width of the sample, reducing its velocity with each "round trip" until it reaches the straight centre which will allow the taper to be created. The velocity of the X-trajectory will then be increased with each "round trip" from the centre of the capillary to account for the taper on the opposite side. The acceleration gradient of the Y-trajectory will be less towards the centre of the profile to create the required semi-circular profile.

4 Results

A sample of Alumina (ceramic Aluminium Oxide) was micromachined using the femtosecond laser system in order to test the effect of varying the lasers average power. The XPS motion controller was used to ablate small sections of the alumina block in 1mm increments across the edge of the sample. The power of the laser was varied for each increment in order to find an optimum setting. The desired depth is 140 μm as this should form one half of a 280 μm capillary channel. The ablated "trenches" created by laser along the edge of the sample are shown in the optical microscope images of Figure 8.

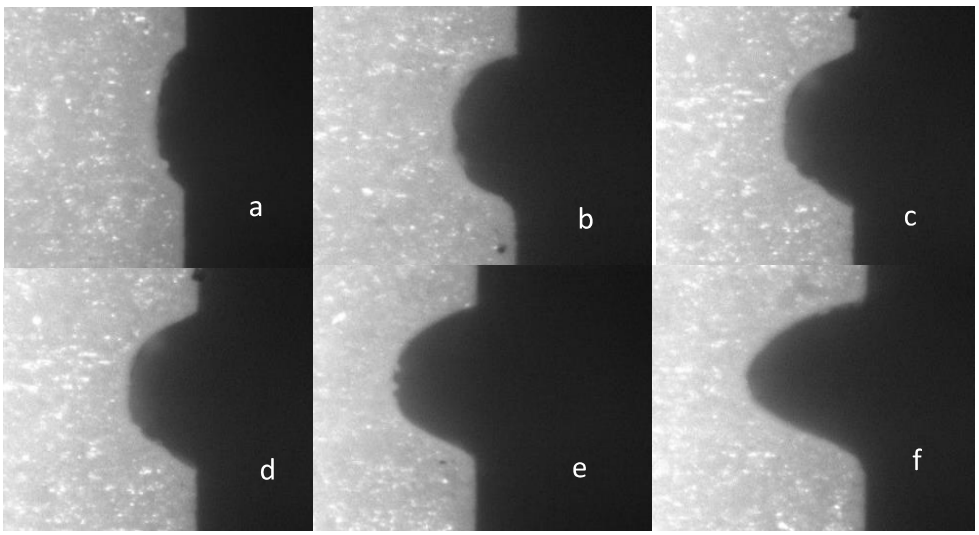

Figure 8 – Images of the 6 micromachined grooves along the alumina sample (lowest (a) to highest (f) power).

It is clear from Figure 8, that as the power of the laser is increased, the profile becomes deeper.
At the highest power (Figure 8 f), it can be observed that the ditch is narrowing with depth, indicating that the power is too high to obtain the desired semi-circular profile.

a) Straight Capillary
Once the two straight capillary plates were machined, they were aligned together using a microscope and glued using epoxy glue. The diameter of the capillary channel was measured to be 288 μm using the optical microscope which is close to the nominal value of 280 μm expected from the trajectory program used to machine it. The diameter of the straight capillary is shown in Figure 9 in which the degree of circularity is seen to be very high.

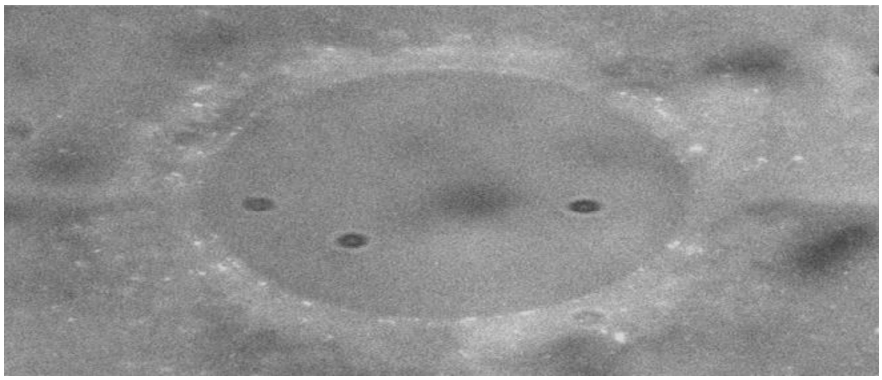

Figure 9 – Image of the end of the straight capillary using the optical microscope (the black circles are merely specks of dirt on the lens of the microscope).

b) Tapered Capillary
The each side of the tapered capillary was machined using the femtosecond laser in the micromachining station. The taper of the capillary was analysed using the optical microscope to image along the length of the 4cm capillary in 2mm intervals. A profile of the tapered capillary channel is shown in Figure 10.

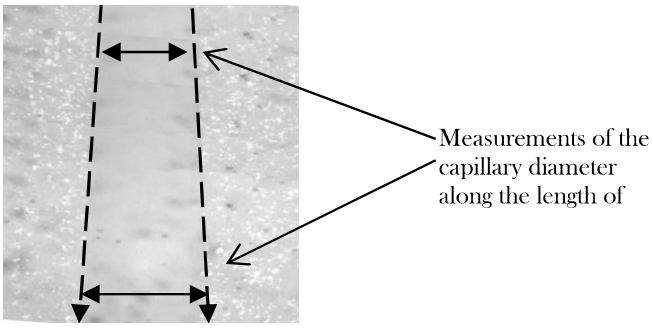

Figure 10 – Compiled images of sections measured at 2mm intervals along the capillary length showing the taper from the wide to the narrow side.

The diameter along the semi-circular profile was recorded for each 2 mm increment along the length of the capillary. This was repeated for the other capillary plate to ensure that both plates had been correctly machined and their tapers even. The profiles of each side of the tapered capillary are shown in the Figure 11.

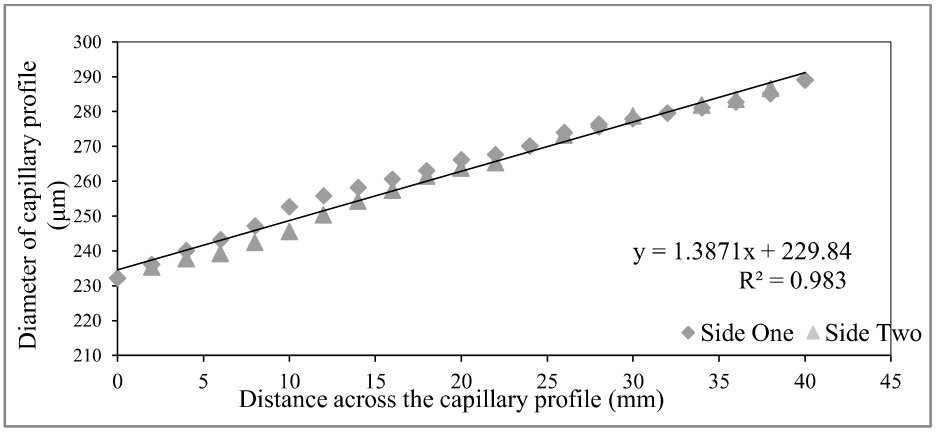

Figure 11 – Varying diameter of the tapered capillary profile across the length of the capillary. Graph displays the measurements of each capillary plate in which both have a linear taper.

From Figure 11, it is clear that the taper of the capillary is linear and tapers from 289 µm to 232 µm. The discrepancies between the sides are mainly caused by the inaccurate measurement of the width of the capillary channel using "Image J" software. Figure 12 displays images of both ends of the capillary one it was glued together. The tapering is clearly observed by the change in diameter of the circular profile.

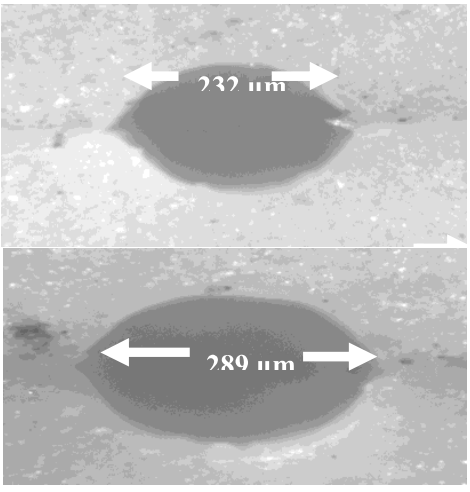

Figure 12 – Images of each of the tapered capillary ends showing change in diameter.

5 Discussion of Results

The laser imaging system successfully located the focus of the helium neon laser and the femtosecond laser beam. The straight capillary had a constant diameter of 288 μm . The two ends of the tapred capillary were measured to have diameters of 232 μm and 289 μm and a linear taper along the length of the channel as shown in Figures 11 and 12. The degree of tapering to be used will of course be determined by the final requirements of the applied experiments.

6 Conclusion

The channel is formed by machining semi-circular channels of diameter d into two alumina (ceramic) or sapphire (crystalline) blocks, which are then carefully sandwiched together to form a narrow capillary of length L. These materials have high electrical resistivity, high dielectric strength, high thermal conductivity and impressive thermal stability. Therefore, because of the excellent insulation properties, they are very reliable materials in high-power electronics. However, due to their hardness, it is difficult and expensive to machine. Femtosecond micromachining allows large band-gap materials, such as these, to be machined with minimal thermally and mechanically produced defects. The ablative characteristics of the femtosecond laser system were explored and micromachining of both the straight and tapered capillary waveguides was successful. Femtosecond laser micromachining is an effective technique for producing channels and appropriate acceleration of the scanning machining laser enables the formation of a linear tapered capillary cross-section.

7. References

[1] Bingham, R. (2006) 'Basic concepts in plasma accelerators', Philosophical Transactions of the Royal Society a-Mathematical Physical and Engineering Sciences, 364(1840), 559-575.
[2] Vieux, G. (2004) 'Broad-band linear Raman chirped pulse amplification in plasma', PhD Thesis, Department of Physics, University of Strathclyde, Glasgow.
[3] Esarey, E., Schroeder, C. B. and Leemans, W. P. (2009) 'Physics of laser-driven plasma-based electron accelerators', Reviews of Modern Physics, 81(3), 1229-1285.
(4) Jaroszynski, D. A., Bingham, R., Cairns, R. A. (2009), "Laser-Plasma Interactions", CRC Press, Boca Raton, 101-142.
[5] Rowlands-Rees, T. P. et al. (2008) 'Laser-driven acceleration of electrons in a partially ionized plasma channel', Physical Review Letters, 100(10).
[6] Jaroszynski, D. A. et al. (2006) 'Radiation sources based on laser-plasma interactions', Philosophical Transactions of the Royal Society a-Mathematical Physical and Engineering Sciences, 364(1840), 689-710.
[7] Geddes, C. G. R. et al. (2004) 'High-quality electron beams from a laser wakefield accelerator using plasma-channel guiding', Nature, 431(7008), 538-541.
[8] Leemans, W. P. et al. (2006) 'GeV electron beams from a centimetre-scale accelerator', Nature Physics, 2(10), 696-699.

[9] Spence, D. J., Butler, A. and Hooker, S. M. (2003) 'Gas-filled capillary discharge waveguides', Journal of the Optical Society of America B-Optical Physics, 20(1), 138-151
[10] Gamaly, E. G., Rode, A. V., Luther-Davies, B. and Tikhonchuk, V. T. (2002) 'Ablation of solids by femtosecond lasers: Ablation mechanism and ablation thresholds for metals and dielectrics', Physics of Plasmas, 9(3), 949-957.
[11] Wiggins, S.M. (2010) Advanced Topics in Optics Class Lecture, University of Strathclyde, Glasgow.
[12] Guizard, S. et al. (2002) 'Femtosecond laser ablation of transparent dielectrics: measurement and modelisation of crater profiles', Applied Surface Science, 186(1-4), 364-368.
[13] Bobrova, N. A. et al. (2002) 'Simulations of a hydrogen-filled capillary discharge waveguide', Physical Review E, 65(1).
[14] Jaroszynski, D. A. et al. (2000) 'The Strathclyde terahertz to optical pulse source (TOPS)', Nuclear Instruments & Methods in Physics Research Section a-Accelerators Spectrometers Detectors and Associated Equipment, 445(1-3), 317-319.
[15] Newport, XPS Controller User Manual, Documentation V2.1.0